Second-harmonic microscopy for fluence-dependent investigation of laser-induced surface reactions

K. Klass,[1] G. Mette,[1] J. Güdde,[1] M. Dürr,[1,2] and U. Höfer[1]

[1]*Fachbereich Physik und Zentrum für Materialwissenschaften, Philipps-Universität, D-35032 Marburg, Germany*

[2]*Fakultät Angewandte Naturwissenschaften, Hochschule Esslingen, D-73728 Esslingen, Germany*

(Received 1 October 2010; revised manuscript received 12 January 2011; published 25 March 2011)

Spatially resolved optical second-harmonic generation (SHG), that is, SHG microscopy, is shown to be a versatile tool for the investigation of femtosecond laser-induced surface processes such as adsorbate diffusion and desorption and their dependence on absorbed laser fluence. As an example, time-resolved measurements on the diffusion of O from the steps onto the terraces of a vicinal Pt(111) surface at low substrate temperature were performed. Using the sensitivity of SHG on step coverage and analyzing the signal change across the laser beam profile via SHG microscopy during laser-induced diffusion, the strong nonlinear fluence dependence of the diffusion rate could be determined. Using SHG microscopy in combination with a two-pulse correlation scheme, time-resolved information on the surface reaction was obtained as a function of absorbed laser fluence.

DOI: 10.1103/PhysRevB.83.125116 PACS number(s): 82.53.St, 42.65.Ky, 68.43.Jk, 78.47.J−

I. INTRODUCTION

High-intensity femtosecond laser pulses can efficiently induce reactions such as desorption, dissociation, or diffusion on metal surfaces.[1,2] The reactions are typically based on photoexcitation of hot electrons in the metal substrate, which couple to nuclear motion and lead to desorption, dissociation, or diffusion of adsorbed species. In the case of the early experiments on desorption induced by electronic transitions (DIET),[3–6] the reaction is initiated by single electronic transitions. Due to the short lifetime of the electronic excitation at the surface, these processes are typically very inefficient. The reaction yield can be drastically enhanced using femtosecond laser pulses, which induce a high density of electronic excitation at metal surfaces.[7–22] Repetitive transitions between ground and excited state of the respective potential energy surface are then possible during the adsorbate's movement on the surface.[23] As a consequence, such desorption induced by multiple electronic transitions (DIMET) shows a strong nonlinear dependence on absorbed laser fluence.[7,11,19]

This nonlinear fluence dependence provides important information on the underlying photochemical processes.[11,22] Moreover, it is the basis for investigations in the time domain by means of two-pulse correlation measurements.[8] For this purpose, the reaction yield is measured as a function of a delay between two excitation pulses. If the system maintains memory of the first excitation, the second pulse can couple to this excitation and an enhanced reaction yield compared to the single excitation will be observed due to the high nonlinearity of DIMET processes. The width of the two-pulse correlation thus contains information on the time scale on which energy is transferred from the electronic excitation to the adsorbate degrees of freedom and allows, for example, for the distinction between electron- and phonon-mediated processes.[10,14]

The typical experimental procedure in desorption experiments makes use of quadrupole mass spectrometry (QMS) to analyze the products of the photoinduced reaction. Since these reaction products are collected from the whole area illuminated by the laser spot, depending on the laser profile, areas of very different local laser fluence are probed and averaged within one experiment. Under these circumstances, the correct dependence of the reaction rate on absorbed laser fluence cannot be determined directly from the experiment. Frequently, it is deduced by means of a self-consistent modeling based on a yield-averaged laser fluence.[2,13,15] Although QMS in combination with yield-averaging techniques is capable of accounting for the correct fluence dependence of the reaction rate, such iterative procedures cannot be applied for the evaluation of two-pulse correlations. Thus the result reflects an average over the fluence distribution of the laser spot. In contrast, recent measurements of laser-induced diffusion used optical second-harmonic generation (SHG) as a probe.[19,20,24,25] With a probe beam that is small compared to the pump, this technique enables experiments at well-defined laser fluences. No modeling is required to deduce the fluence dependence, and the result of two-pulse correlation measurements corresponds to a well-defined laser fluence. In the case of laser-induced diffusion of CO on Pt, for example, it has been shown by the SHG technique that two-pulse correlation narrows substantially when the laser fluence is decreased.[20]

In the present work, we extend the SHG technique for time-domain studies of laser-induced surface reactions with an optical microscopy setup.[26,27] Analyzing the spatially resolved SH response from the surface, we exploit the intensity variation across the profile of the laser pulse to extract the information on the dependence of the reaction rate on applied laser fluence. With this technique, two-pulse correlation measurements can be performed systematically and routinely as a function of absorbed laser fluence. As an example, we report studies of laser-induced diffusion of oxygen on a vicinal platinum surface at low substrate temperatures. The O/Pt system is a model system for chemisorption on metal surfaces.[28,29] Previous studies of laser-induced diffusion have exploited the enhanced reactivity of step sites[19,24] in a similar way as thermally activated diffusion of hydrogen has been observed on vicinal silicon surfaces.[30,31] At low substrate temperatures, oxygen dissociation proceeds preferentially at the top of the step edges.[32] As a result, the step sites are selectively saturated with oxygen atoms in the presence of clean terraces. Diffusion of oxygen from the step sites onto the terraces is then induced by means of femtosecond laser pulses and detected by a changed SH response of the surface.

II. EXPERIMENTAL PROCEDURE

In our experiment, the same femtosecond pulses were used both to induce the diffusion process as well as to generate second-harmonic light (see Fig. 1). The measurements were conducted under ultrahigh-vacuum (UHV) conditions at a base pressure below 10^{-10} mbar using a Pt(997) surface, that is, a vicinal Pt(111) crystal with steps oriented perpendicular to the $[11\bar{2}]$ direction (B-type). Standard sputtering and annealing cycles in combination with oxygen treatment were used to clean the sample.[24] As a result, scanning tunneling microscopy (STM) images of the surface showed regular monatomic steps separating terraces with a mean width of about nine atomic rows. Molecular oxygen was dosed via a gas-dosing system, and the gaseous flux was controlled by measuring the background pressure. At all times, the oxygen pressure was below 10^{-8} mbar. During oxygen dosage, the sample was held at 150 K by means of liquid-nitrogen cooling, and the increasing step coverage was determined by measuring the integrated second-harmonic signal. It has been previously shown that these dosing conditions lead to selectively saturated step sites. Using p-polarized light and by orienting the steps with an azimuthal angle of 60° to the plane of incidence, the SH signal shows a high sensitivity on the step coverage comparable to Ref. 24. After each measurement cycle, the sample was flashed to 1000 K to remove the oxygen and cooled down before starting a new cycle.

The optical setup was based on an kHz Ti:sapphire laser system (FEMTOPOWER PRO) that generates laser pulses with a temporal duration of 50 fs at a central wavelength of 800 nm. The beam was slightly focused on the sample with

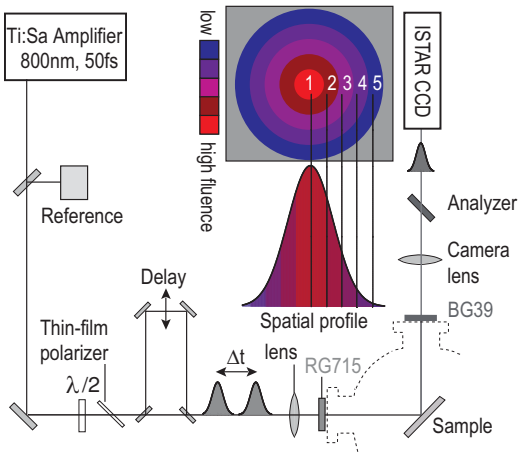

FIG. 1. (Color online) Experimental setup: fs-laser pulses are generated by a Ti:sapphire amplifier; a thin-film polarizer in combination with a $\lambda/2$ plate enables the continuous variation of the peak fluence on the sample. The 800-nm pulses are slightly focused on the sample; the specular reflected p-polarized component of the SH light is imaged by means of a camera lens on the CCD camera. An interferometer containing a delay stage allows for two-pulse correlation measurements. For illustration of the experiment, an intensity distribution across the spot profile and the resulting spatial distribution of laser fluence on the sample is sketched as well. Analyzing regions (1) to (5) of the spatially resolved SH signal will give information on the fluence dependence of the investigated process.

an angle of incidence of 45° from the surface normal. This led to an average spot diameter of 420 μm [full width at half-maximum (FWHM)]. The absorbed peak fluence could be varied between 0 and 7 mJ/cm^2 by a combination of a half-wave plate and a thin-film polarizer. During the adsorption process, the absorbed peak fluence was kept below 2.4 mJ/cm^2 to prevent the activation of laser-induced diffusion. After the adsorption process, the laser was blocked and the absorbed peak fluence of the laser beam was increased to values between 4.0 and 5.7 mJ/cm^2 to induce the hopping process. Both adsorption and diffusion were monitored by detecting the specular reflected SH signal, which was generated by the incident laser beam.

For this purpose, we separated the p-polarized SH component from the fundamental wave using an analyzer, a BG39 filter, and a number of dielectric 400-nm mirrors, and we imaged the SH spot optically magnified by a camera lens (NIKON NIKKOR, 1 : 2.8 ED, $f = 180$ mm) on an intensified charge-coupled-device (CCD) chip (ANDOR ISTAR DH720) with a size of 1024 × 256 pixels; each pixel covers an area of 26 × 26 μm^2 on the chip. A microchannel plate in front of the 16-bit camera enables the amplification of the weak SH signal up to four orders of magnitude. For all measurements, the camera was operated at maximum gain, the gate width was 11 ns, and it was triggered externally by the laser. The camera is sensitive in a spectral range from 180 up to 850 nm and was operated in full image mode, which led to minimum readout times of 2 μs/pixel. To measure a two-pulse correlation, the p-polarized laser beam was split and two beams of approximately the same fluence were combined collinearly on the sample with the introduction of a variable time delay.

The absorbed fluence in selected areas of the spot was determined by taking into account the optical constants of platinum,[33] the magnification by the camera lens, as well as the quadratic dependence of the generated SH signal on the absorbed power in combination with the measurement of the integrated laser power. In detail, the total absorbed power $P_{\mathrm{abs,total}}$ is calculated by the averaged laser power P, which is measured by a conventional power meter in front of the UHV chamber, the transmission coefficient of the UHV window $\tau_{\mathrm{window}} = 0.92$, and the absorption coefficient $\alpha = 0.372$ of the sample for p-polarized light at the realized angle of incidence:[33]

$$P_{\mathrm{abs}} = P\tau_{\mathrm{window}}\alpha.$$

Due to the functional dependence of the SH yield I on the absorbed power,

$$I \propto P_{\mathrm{abs}}^2,$$

we relate the total power absorbed by the sample to the sum over the root of the counting rate each pixel contains:

$$P_{\mathrm{abs,total}} \propto \sum_{k=1}^{N_{\mathrm{total}}} \sqrt{I} = \Sigma_{\mathrm{total}}.$$

For selected regions, for example, elliptical rings with comparable local laser fluence (see below), the square root of the signal within all pixels of the region is summed up. For the

absorbed power in the selected area,

$$P_{\mathrm{abs,area}} \propto \sum_{k=1}^{N_{\mathrm{area}}} \sqrt{I} = \Sigma_{\mathrm{area}}$$

applies, N_{area} being the number of selected pixels. By taking into account the size of the projection of one CCD pixel on the sample, A_{pixel}, which is given by the magnification $M = 7.7$ of our setup and the pixel's size on the CCD chip, the area of a chosen region on the sample is then calculated by $A_{\mathrm{area}} = A_{\mathrm{pixel}} N_{\mathrm{area}}$. Finally, the resulting fluence is determined from the ratio of Σ_{area} and Σ_{total}, taking into account the absorbed power $P_{\mathrm{abs,total}}$, the laser's repetition rate $f_{\mathrm{rep}} = 1$ kHz, and A_{area}. In the experiment, we measured the total laser power P with an absolute uncertainty of $\approx 5\%$. We estimate an additional systematic error of $\approx 3\%$ due to the determination of the magnification. Relative changes between single measurement cycles could be determined by the reference arm better than 2%. Because of fluctuations within the spatial extension of the spot, we estimate that the values of our fluence data vary with a statistical error of 3%.

III. RESULTS

A. Fluence dependence

A typical experimental cycle is depicted in Fig. 2. The upper panel displays the integrated SH signal normalized with respect to the high-fluence signal of the clean surface. The lower panel shows selected images of a sequence of images that has been taken by the CCD camera. The moment when an image has been recorded by the CCD chip is indicated by arrows in the upper panel of the figure. First, a comparatively small peak fluence of 2.4 mJ/cm^2 is used to monitor the adsorption process (images 1–3); the signal decreases rapidly with oxygen dosage and saturates on a low level. For a short time, the laser is blocked to increase the laser power. Starting with image (4), the laser has been unblocked; the signal increases rapidly due to laser-induced diffusion and saturates at a signal intensity close to the initial signal of the clean surface at high fluence (images 4–6). To maximize the signal-to-noise ratio, an exposure time of 3 s was used for all measurements, followed by 1 s read-out time. Comparing images (1–3) with (4–6) in Fig. 2, a change of the SH spot profile after laser-induced diffusion can be easily identified. The spot profile is much steeper in image (6) when compared to image (1), thus indicating the strong nonlinear dependence of laser-induced diffusion on laser fluence.

For a quantitative evaluation, the spatially resolved SH signal was divided into areas of similar laser fluence. A first, rather simple geometric approach is displayed in Fig. 3: The upper panel shows the SH spot from the clean surface as a false color intensity plot. Elliptic areas of similar initial intensity were fit to the spot profile and are hatched in gray. The SH signal within these selected areas is summed up and normalized to the number of selected pixels. Comparison of the SH signal from the clean surface with the signal from the surface with fully occupied step edges has been used to relate the SH signal to the relative step coverage assuming a linear relation between the nonlinear susceptibility and the step coverage, as discussed in Refs. 20 and 24. The resulting step

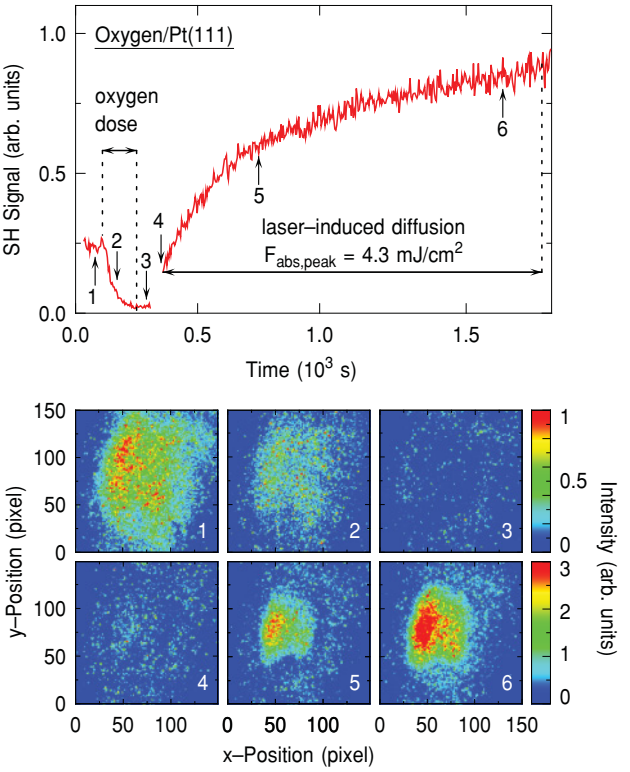

FIG. 2. (Color) Upper panel: Integrated second-harmonic response of the Pt sample as a function of time during dissociative adsorption of O_2 at the steps (oxygen dose) and diffusion of atomic oxygen induced by femtosecond laser pulses. For the laser-induced diffusion, the peak laser fluence was increased from 2.4 to 4.3 mJ/cm^2. Lower panel: Sequence of false color plots of the generated SH spot, which is recorded by the intensified CCD camera during adsorption (1–3) and diffusion (4–6). Note the different scale for images (1–3) and (4–6). Arrows in the upper panel indicate the time when the respective images in the lower panel have been recorded by the CCD camera.

coverage and its depletion as a function of applied laser shots is displayed in the lower panel of Fig. 3. The repetitive excitation of the surface at a rate of 1 kHz leads to a continuous depletion of the step sites, which is faster the closer the inspected area is to the center of the spot. From the temporal change in the step coverage, hopping probabilities per laser shot for oxygen diffusion from the fully occupied steps onto the terraces were determined using a one-dimensional rate equation model.[24] This model is able to describe the experimental data over the whole coverage range for low as well as for high fluences. The fits of the model to the data are drawn as solid lines in the lower panel of Fig. 3. In Fig. 4, the resulting hopping rates are plotted as a function of absorbed laser fluence.

Within the geometrically chosen areas, pixels with different initial intensities are still analyzed as an ensemble, consequently areas with smaller and higher hopping rates are evaluated together. The influence of this effect depends on the quality of the laser profile as well as on the functional dependence of the investigated effect on laser fluence. To better account for this situation, we applied a second method of analysis: single pixels showing an initial signal intensity in a chosen intensity interval were combined for the evaluation,

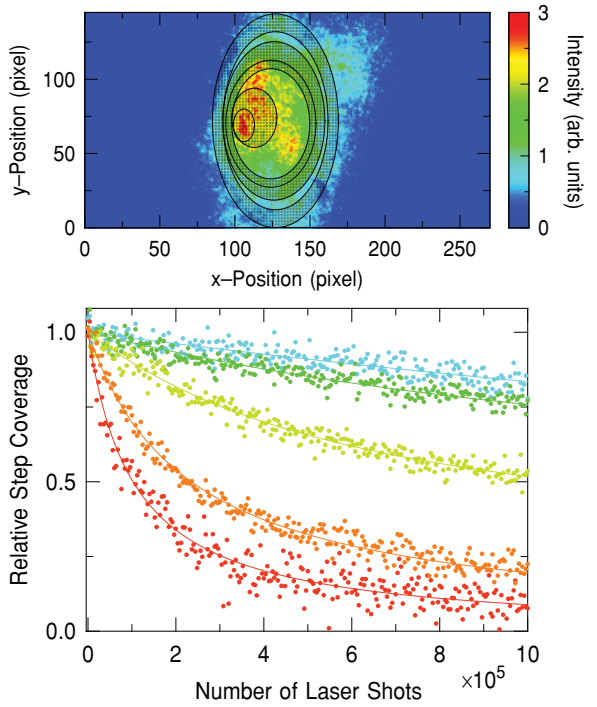

FIG. 3. (Color) Upper panel: Spatially resolved SH signal as intensity false color plot, selected areas are hatched in gray. The peak fluence in the center was $F_{\text{abs}} = 4.9$ mJ/cm^2. Lower panel: Relative step coverage of oxygen as a function of applied laser shots for the selected areas (inner area: $F_{\text{abs}} = 4.9$ mJ/cm^2, high depletion rate; outer areas: $F_{\text{abs}} = 2.7$ mJ/cm^2, lower depletion rate). Fits are drawn as solid lines.

regardless of their actual position on the chip. For this purpose, first the intensity distribution of the SH spot generated by the clean surface at high fluences was recorded. The distribution was then divided into intervals. The interval size was typically chosen large enough to obtain a sufficient signal-to-noise ratio but small enough not to average over a too large range of laser fluence; for example, in the center of the spot, 80 pixels are adequate to form a suitable area of comparable fluence, while the interval size in outer areas is typically larger. The integrated signal within these ensembles of pixels (bins) is analyzed, and hopping probabilities per laser shot are determined as described above. The results are plotted as empty symbols in Fig. 4. They are in good quantitative agreement with the results of the simple geometric approach, which is apparently sufficient in our case. Depending on laser profile quality, we recommend the more advanced binning procedure to use the SHG microscopy to full capacity.

In our experiment, a fluence range from ≈ 3 to 6 mJ/cm^2 was analyzed; in this range, the hopping rates show a strong nonlinear dependence on the fluence. The double-logarithmic plot (inset of Fig. 4) indicates that in this fluence range, the data can be described by a simple power law for the dependence of the hopping probability per laser shot on the absorbed laser fluence F_{abs}. A respective linear fit reveals a dependence $\propto F_{\text{abs}}^{6-7}$ as illustrated by the solid line in both the main panel and the double-logarithmic plot in the inset of Fig. 4.

The direct observation of the optically resolved SH spot enables us to control the spatial stability of the laser spot on

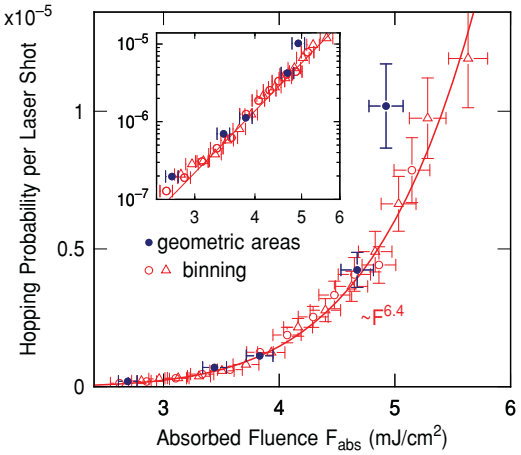

FIG. 4. (Color online) Fluence dependence of the extracted hopping probabilities per laser shot of O from fully occupied steps onto the initially empty terraces of the vicinal Pt(111) surface induced by fs-laser pulses. Hopping rates obtained by a geometrical division of the spot are shown as filled dots, data obtained by the binning procedure are shown as open symbols. Data points indicated by the same symbol belong to one single measurement. The inset displays the same data in a double logarithmic scale. The solid lines depict a power law $\propto F_{\text{abs}}^{6.4}$.

the sample. Since one measurement cycle lasts approximately 20 min, small lateral movements on the sample were observed, which are most likely caused by thermal expansion of the cooled sample holder. When we analyzed lateral movements of the spot on the sample up to 35 μm, no influence on the functional dependence of the hopping rate on the fluence was found. This might be explained by the fact that the data most relevant for the determination of the hopping probability per laser shot are taken on a much smaller time scale of only a few tens of seconds.

B. Two-pulse correlation

The nonlinear dependence of the hopping rates on the absorbed laser fluence is the prerequisite for the application of a two-pulse correlation (2PC) scheme,[8] which makes it possible to analyze the dynamics of the energy transfer between the initially excited electrons and the adsorbates. For this purpose, an interferometric delay stage was installed in the setup to split up the laser pulse into two parts. Diffusion is then induced for different time delays between both beams, and the hopping probabilities per laser shot are determined as a function of time delay. If the SH signal is detected with spatial resolution using the microscopy setup, fluence-dependent information on the width of the 2PC can be obtained.

For a quantitative evaluation, again the geometric approach was applied to divide the spot into areas of comparable fluence. Hopping probabilities per laser shot were determined within the 2PC scheme applying absorbed fluences in the range of 4.2–6.9 mJ/cm^2, split into two beams of comparable intensity ($p + p$ polarization). The weaker beam precedes the stronger for negative delays; the results are summarized in Fig. 5. Because of interferences between both laser beams around zero delay, no data were measured between -130 and 130 fs. Lorentz functions were applied to empirically fit the obtained

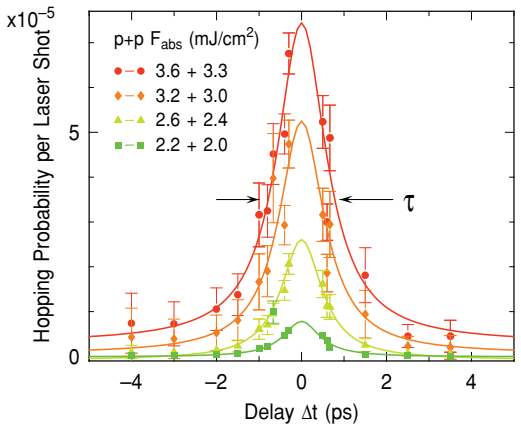

FIG. 5. (Color online) Two-pulse correlation traces (data points) for different absorbed fluences; for negative delays, the weaker beam precedes the stronger one. Solid lines show Lorentzian functions fitted to the experimental data to determine the width τ of the 2PC. For the highest fluence combination, the FWHM $\tau = 1.4$ ps is indicated by the arrows.

data; the widths are in the range between 1.0 and 1.4 ps and increase with increasing fluence. The obtained widths are plotted as a function of laser fluence in Fig. 6.

IV. DISCUSSION

Using SH microscopy for the observation of laser-induced surface processes, we introduced a technique to simplify the study of the typically nonlinear fluence dependence of such processes when induced by multiple electronic transitions. In the case of laser-induced diffusion of oxygen on vicinal

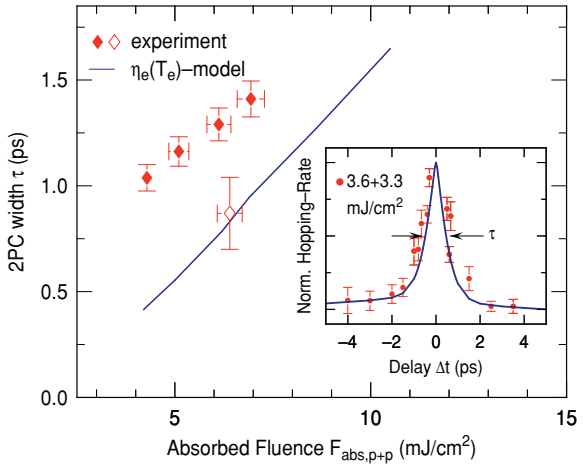

FIG. 6. (Color online) FWHM τ of the 2PC shown in Fig. 5 as a function of absorbed laser fluence (filled data diamonds). In comparison, the results from simulations using the empirical friction model of Ref. 25 with a friction coefficient of the form $\eta_e = \eta_0 T_e^2$ and a diffusion barrier $E_{diff} = 0.8$ eV are drawn as a solid line. Additionally, the FWHM obtained when averaging the SH response over the whole spot is shown (empty diamond, see main text). Inset: 2PC measurement in the center part of the laser spot (filled circles) and modeled 2PC (line) normalized for the same offsets and peak maxima.

platinum, a strongly nonlinear dependence of the hopping probability per laser shot on the absorbed laser fluence of the form $\propto F^{6-7}$ was observed within one single experiment in the range between 2 and 6 mJ/cm^2. Although the observed fluence dependence is similar to the results of earlier experiments on laser-induced desorption[7,13,34,35] and diffusion,[20] it shows a weaker dependence on laser fluence compared to results reported for laser-induced diffusion of oxygen on vicinal Pt(111) from our own group.[19] However, it has to be noted that we used a vicinal Pt surface with monatomic steps of type B, whereas in the earlier experiment, steps of type D were investigated, which might be associated, for example, with a higher diffusion barrier.

As a main advantage of SHG microscopy in femtochemistry, we were able to measure fluence-dependent two-pulse correlations for the laser-induced diffusion of oxygen on vicinal Pt(111). For laser-induced processes, the width of the 2PC allows us to distinguish between electron- and phonon-mediated processes;[2] furthermore, it is often used to estimate the time scale on which the energy flows from the optically excited electron system to the adsorbate. In our experiment, the small width of 1.0–1.4 ps for the investigated range of absorbed fluence is a clear indication for the electron-mediated process and is in good agreement with earlier results.[19] As a consequence of the dependence of the width of the 2PC on the absorbed laser fluence, it is not possible to directly identify a single transfer time with that width.[20] Indeed, the broadening of the 2PC with higher fluence is a general phenomenon for laser-induced processes and can even be understood in a very simple picture, for example, by means of the empirical friction model using a constant friction coefficient.[1,36] More sophisticated models take into account the anharmonicity of the potential for the adsorbate motion, which then results in a heat-transfer coefficient that depends on adsorbate temperature.[37]

In the framework of the empirical friction model, electrons, ions, and adsorbate are modeled to be interacting heat baths with time-dependent temperature distributions. The adsorbate temperature T_a is coupled via an electronic friction coefficient η_e to the electron temperature. The reaction rate is then given by an Arrhenius-type expression of the form $R(t) = k_0 \exp[-E_{diff}/k_B T_a(t)]$, where k_0 is a constant prefactor and the time integral $p = \int R(t)dt$ corresponds to the hopping probability per laser shot. This exponential dependence of the rate on adsorbate temperature is the main reason for the broadening of the 2PC with increasing fluence: at higher laser fluence, the system stays longer at a given temperature T_a necessary for efficient coupling of the second pulse of a 2PC experiment. A reduced increase in T_e with higher laser fluence due to the nonlinear dependence of $T_{e,max}$ on laser fluence further enhances this effect. The phenomenon has been discussed in detail in Ref. 20 for the diffusion of CO on platinum.

In the case of oxygen diffusion on Pt(111), fluence dependence and width of 2PC measurements cannot be modeled consistently with a constant friction coefficient η_e, most likely because of an indirect excitation mechanism.[19] It has been proposed that the hot electrons primarily excite O-Pt vibrations, which then couple to the frustrated translations required to initiate lateral motion.[19,37–39] As an approximation of the resulting nonlinear coupling, Stépán *et al.*[19] introduced

an empirical dependence of η_e on electron temperature. Figure 6 illustrates that this model is consistent with the observed broadening of the 2PC with increasing laser fluence. For the calculations, we use the same quadratic temperature dependence of η_e as in our previous work.[19,25] As discussed before, this model predicts a narrower 2PC than the experiment. The presented results show that the underestimation of the measured widths becomes even stronger for lower laser fluences. The overall trend of the fluence-dependent width of the 2PC obtained by SHG microscopy, however, is reproduced quite well. Also in the case of a slightly more complex excitation mechanism described by this model, the "threshold temperature" required for appreciable diffusion is reached for a longer time duration at higher laser fluences, which consequently leads to a broader 2PC.

To demonstrate the importance of the fluence-resolved measurement of the 2PC, we have also analyzed the SHG response averaged over the whole laser spot. The 2PC width of the averaged data is only 0.87 ps, whereas corresponding yield-averaged fluence amounts to $F_{\mathrm{abs,yield}} = 6.4$ mJ/cm^2. The true width of the 2PC for this fluence can be determined by interpolating between actually measured widths for fluences of 6.2 and 6.9 mJ/cm^2 (Fig. 6). It is 1.34 ps and thus considerably larger than the width of the averaged data. This discrepancy can be understood intuitively by the fact that the yield-averaged fluence is close to the maximum fluence whereas the contributions to the 2PC from outer parts of the beam profile results in a smaller width of the 2PC for the whole spot compared to the width of the laterally resolved 2PC for the inner parts. Consequently, the analysis of a 2PC experiment without lateral resolution can significantly underestimate the time scale for energy transfer or assign a considerably higher electronic friction coefficient to femtosecond laser-induced processes.

Finally, we will discuss the applicability of SHG microscopy for the investigation of femtochemical processes in general. In the present work, we used SHG to detect diffusion by taking advantage of its sensitivity on step coverage. However, as long as the SH signal can be related to the reaction yield, SHG can be used for all kinds of surface reactions, for example, for desorption, and both on vicinal and flat surfaces. The relation between the SH signal and surface coverage has to be calibrated, which might be seen as a disadvantage of the method, especially if the relation is nonlinear. However, such a calibration was successfully applied for various adsorbate systems, for example, for hydrogen on silicon surfaces.[40] Although a QMS directly detects the desorbing molecules without the necessity of a calibration, the investigation of desorption using SHG has the great advantage of a very high sensitivity. This makes it possible to investigate surface reactions even for very small concentrations of adsorbates. With our setup, we were able to detect step-diffusion rates down to 10^{-7} per laser shot for a step density of only one step atom per nine terrace atoms. The high sensitivity results mainly from the fact that the SH signal can be monitored over many laser shots, independent of the reaction rate, whereas a QMS detection requires a minimum number of desorbing molecules per shot. The combination of SHG detection with lateral resolution, by means of SHG microscopy, enables the investigation of a broad fluence range at once with a high dynamic range. The lateral resolution makes it possible to perform time-domain studies at well-defined fluences, which is essential to gain reliable information about the energy transfer between substrate and adsorbate. For this application, the use of a 2PC scheme has the advantage that the form of the correlation function is not influenced by transient changes of the optical properties of the substrate, which often dominate the time-resolved traces of pump-probe experiments.

V. SUMMARY

In summary, we have introduced SHG microscopy as a method to analyze femtosecond laser-induced processes on surfaces and their fluence dependence within one measurement. In particular, with this method we were able to measure the width of two-pulse correlations for different, well-defined fluences, which is a prerequisite for a detailed analysis of the data. We demonstrated the advantages of SHG microscopy by studying laser-induced diffusion of O from the step edges onto the terrace site of a vicinal Pt(111) crystal in a fluence regime of $F_{\mathrm{abs}} = 2$–6 mJ/cm^2. A nonlinear dependence of the hopping rate on the laser fluence was confirmed for the O/Pt(111) system; in the investigated fluence range, we found a power law of the fluence dependence of $\propto F_{\mathrm{abs}}^{6-7}$. Two-pulse correlation measurements revealed an almost linear dependence of the 2PC width on the laser fluence with values between 1.0 and 1.4 ps. Finally, SHG microscopy with its advantages is not limited to laser-induced diffusion experiments, and broader application in femtochemistry is encouraged.

ACKNOWLEDGMENTS

Funding by the Deutsche Forschungsgemeinschaft through Graduate School 790 is gratefully acknowledged.

[1] J. A. Misewich, T. F. Heinz, P. Weigand, and A. Kalamarides, in *Laser Spectroscopy and Photo-Chemistry on Metal Surfaces, Part II*, edited by H. L. Dai and W. Ho (World Scientific, Singapore, 1996), pp. 764–826.

[2] C. Frischkorn and M. Wolf, Chem. Rev. **106**, 4207 (2006).

[3] D. Menzel and R. Gomer, J. Chem. Phys. **41**, 3311 (1964).

[4] P. A. Redhead, Can. J. Phys. **42**, 886 (1964).

[5] E. Hasselbrink, Chem. Phys. Lett. **170**, 329 (1990).

[6] X. L. Zhou, X. Y. Zhu, and J. M. White, Surf. Sci. Rep. **13**, 73 (1991).

[7] J. A. Prybyla, T. F. Heinz, J. A. Misewich, M. M. T. Loy, and J. H. Glownia, Phys. Rev. Lett. **64**, 1537 (1990).

[8] F. Budde, T. F. Heinz, M. M. T. Loy, J. A. Misewich, F. de Rougemont, and H. Zacharias, Phys. Rev. Lett. **66**, 3024 (1991).

[9] J. A. Prybyla, H. W. K. Tom, and G. D. Aumiller, Phys. Rev. Lett. **68**, 503 (1992).

[10]J. A. Misewich, T. F. Heinz, A. Kalamarides, U. Höfer, and M. M. T. Loy, J. Chem. Phys. **100**, 736 (1994).
[11]D. G. Busch and W. Ho, Phys. Rev. Lett. **77**, 1338 (1996).
[12]T. H. Her, R. J. Finlay, C. Wu, and E. Mazur, J. Chem. Phys. **108**, 8595 (1998).
[13]L. M. Struck, L. J. Richter, S. A. Buntin, R. R. Cavanagh, and J. C. Stephenson, Phys. Rev. Lett. **77**, 4576 (1996).
[14]M. Bonn, S. Funk, C. Hess, D. N. Denzler, C. Stampfl, M. Scheffler, M. Wolf, and G. Ertl, Science **285**, 1042 (1999).
[15]S. Funk, M. Bonn, D. N. Denzler, C. Hess, M. Wolf, and G. Ertl, J. Chem. Phys. **112**, 9888 (2000).
[16]D. N. Denzler, C. Frischkorn, M. Wolf, and G. Ertl, J. Phys. Chem. B **108**, 14503 (2004).
[17]L. Cai, X. D. Xiao, and M. M. T. Loy, Surf. Sci. **464**, L727 (2000).
[18]L. Bartels, F. Wang, D. Möller, E. Knoesel, and T. F. Heinz, Science **305**, 648 (2004).
[19]K. Stépán, J. Güdde, and U. Höfer, Phys. Rev. Lett. **94**, 236103 (2005).
[20]M. Lawrenz, K. Stépán, J. Güdde, and U. Höfer, Phys. Rev. B **80**, 075429 (2009).
[21]E. H. G. Backus, A. Eichler, A. W. Kleyn, and M. Bonn, Science **310**, 1790 (2005).
[22]M. Mehlhorn, H. Gawronski, and K. Morgenstern, Phys. Rev. Lett. **104**, 076101 (2010).
[23]J. A. Misewich, T. F. Heinz, and D. M. Newns, Phys. Rev. Lett. **68**, 3737 (1992).
[24]K. Stépán, M. Dürr, J. Güdde, and U. Höfer, Surf. Sci. **593**, 54 (2005).
[25]J. Güdde and U. Höfer, J. Phys. Condens. Matter **18**, S1409 (2006).
[26]G. T. Boyd, Y. R. Shen, and T. W. Hänsch, Opt. Lett. **11**, 97 (1986).
[27]K. A. Schultz and E. G. Seebauer, J. Chem. Phys. **97**, 6958 (1992).
[28]H. Wang, R. G. Tobin, D. K. Lambert, C. L. DiMaggio, and G. B. Fisher, Surf. Sci. **372**, 267 (1997).
[29]A. T. Gee and B. E. Hayden, J. Chem. Phys. **113**, 10333 (2000).
[30]M. B. Raschke and U. Höfer, Phys. Rev. B **59**, 2783 (1999).
[31]M. Lawrenz, P. Kratzer, C. H. Schwalb, M. Dürr, and U. Höfer, Phys. Rev. B **75**, 125424 (2007).
[32]P. Gambardella, Ž. Šljivančanin, B. Hammer, M. Blanc, K. Kuhnke, and K. Kern, Phys. Rev. Lett. **87**, 056103 (2001).
[33]*Handbook of Optical Constants of Solids*, edited by E. D. Palik (Academic, San Diego, 1998).
[34]F. J. Kao, D. G. Busch, D. Cohen, D. Gomes da Costa, and W. Ho, Phys. Rev. Lett. **71**, 2094 (1993).
[35]S. Deliwala, R. J. Finlay, J. R. Goldman, T. H. Her, W. D. Mieher, and E. Mazur, Chem. Phys. Lett. **242**, 617 (1995).
[36]F. Budde, T. F. Heinz, A. Kalamarides, M. M. T. Loy, and J. A. Misewich, Surf. Sci. **283**, 143 (1993).
[37]H. Ueba and B. N. J. Persson, J. Phys. Condens. Matter **20**, 224016 (2008).
[38]H. Ueba, M. Hayashi, M. Paulsson, and B. N. J. Persson, Phys. Rev. B **78**, 113408 (2008).
[39]J. Güdde, M. Bonn, H. Ueba, and U. Höfer, in *Dynamics at Solid State Surfaces and Interfaces*, edited by U. Bovensiepen, H. Petek, and M. Wolf (Wiley-VCH, Weinheim, 2010), Vol. 1, p. 409.
[40]M. Dürr and U. Höfer, Surf. Sci. Rep. **61**, 465 (2006).